LA-UR- 97-2777

Approved for public release; distribution is unlimited.

Title: ANOMALOUS WAVE PROPAGATION ACROSS THE SOUTH CASPIAN BASIN.

CONF-970967--

Author(s): KEITH PRIESTLY, UNIVERSITY OF CAMBRIDGE
HOWARD J. PATTON, GEOPHYSICS GROUP EES-3, MS C335, LOS ALAMOS NATIONAL LAB
CRAIG SCHULTZ, LAWRENCE LIVERMORE NATIONAL LAB

Submitted to: PROCEEDINGS OF THE 19TH SEISMIC RESEARCH SYMPOSIUM ON MONITORING A COMPREHENSIVE TEST BAN TREATY.

Los Alamos
NATIONAL LABORATORY

DISCLAIMER

ANOMALOUS WAVE PROPAGATION ACROSS THE SOUTH CASPIAN BASIN

Keith Priestley, University of Cambridge
Howard Patton, Los Alamos National Laboratory[1]
Craig Schultz, Lawrence Livermore National Laboratory[1]
Contract No. F19628–95–K–0017
Sponsored by DOE

ABSTRACT

The Caspian basin blocks the propagation of the regional seismic phase L_g and this has importance consequences for seismic discrimination in the Middle East. Intermediate period surface wave propagating across the basin are also severely affected. In a separate study we have developed a crustal model of the south Caspian basin and the surrounding region. The crust of the basin consists of 15–25 km of low velocity, highly attenuating sediments lying on high velocity crystalline crust. The Moho beneath the basin is at a depth of about 30 km as compared to about 50 km in the surrounding region. In this study we used an idealized rendition of this crustal model to compute hybrid normal mode/finite difference synthetic seismograms to identify the features of the Caspian basin which lead to the seismic blockage. Of the various features of the basin, the thickness and attenuation of the sediments appear to be the dominant blocking mechanism.

Keywords: Caspian basin, surface waves, wave propagation, seismic blockage

[1]This work was performed under the auspices of the Department of Energy by the Lawrence Livermore National Laboratory under contract W-7405-ENG-48 and by the Los Alamos National Laboratory under contract W-7405-ENG-36.

OBJECTIVES

The Caspian basin blocks the propagation of the regional seismic phase L_g and this has importance consequences for seismic discrimination and a Comprehensive Test Ban Treaty. We have recorded broadband regional and teleseismic distance range seismograms at a number of sites around the south Caspian basin. We find that the south Caspian basin also severely disrupts the propagation of intermediate period surface waves. We are studying these data to understand the cause of the blockage.

RESEARCH ACCOMPLISHED

The crust and upper mantle structure of the south Caspian Basin is enigmatic. Early Soviet studies show that the crust of the basin consists of two layers: a thick sedimentary section (15–25 km) with low P-wave velocity (3.5–4.0 km/s) overlying a 12–18 km thick basaltic lower crust. Mangino and Priestley (1997) used teleseismic receiver function analysis to determine the crustal structure at five sites around the south Caspian basin. These models show that the crust in Turkmenia along the trend of the Apshceron–Balkhan Sill — Kopet Dag Mountains is 50 km thick. In the southwestern part of the Caspian basin the crust is 33 km thick and consists of a 13 km thick sedimentary section lying on a high velocity ($V_p \sim 7.1$ km s^{-1}) lower crustal section. In the southeastern part of the basin the crust is 30 km thick and consists of a 10 km thick sedimentary section overlying a 20 km thick low velocity ($V_p \sim$ 5.8 km s^{-1}) crystalline crust. Mangino and Priestley (1997) combined the receiver function models with velocity models from the previous Russian Deep Seismic Sounding results into a ~1800 km long ESE–WNW trending crustal cross–section across the Kura Depression, the south Caspian basin and the Kopet Dag Mountains (Fig. 1). The most significant features of this crustal model are the 20 km variation in thickness of Cenozoic sedimentary basin deposits, the absence of a "granitic" ($V_p \sim$ 5.8-6.5 km s^{-1}) crustal layer in the central part of the south Caspian basin, and a 20 km of crustal thinning beneath the central part of the basin. The Moho beneath the south Caspian basin has a broad arch–like structure whose western boundary is a relatively narrow zone across which the crust thins rapidly (~20 km thinning over a 100 km zone) and whose eastern boundary has a more gradual change in crustal thickness (~20 km thinning over a 400 km zone).

The study of Kadinsky–Cade et al. (1981) demonstrated that the seismic phase Lg is largely blocked for paths crossing the south Caspian Basin. This is clearly demonstrated by the seismograms in Fig. 2 of an earthquake which occurred near the eastern shoreline of the central Caspin Sea. The crust in the vicinity of the epicenter is about 50 km thick (Mangino and Priestley, 1997). The PDE depth for the event is 40 km but because focal depths in this area are not well constrained, it is impossible to tell from this whether the event is in the crust or mantle. Jackson and Priestley (unpublished work) have used waveform modeling to constrain the depth at 45 km placing it in the crust. The seismogram at LNK on the southwestern coastline shows an impulsive S_n phase but little energy in the L_g group velocity window. The crust between KRF near the epicenter and ABKT has nearly a uniform thickness of 50 km. The seismogram of the event at ABKT show an S_n and L_g phase typical of that seen on stable continental paths. The seismogram at KAT near the southeastern coastline is anomalous. There is a clear S_n phase which is followed by a high amplitude long duration coda. These three seismograms demonstrate the challenge in using regional phases in this region for seismic discrimination.

New seismic data shows that the south Caspian Basin also severely disrupts intermediate frequency (0.017 – 0.10 Hz) fundamental mode surface wave trains (Fig. 3). This effect is observed for surface waves propagating along both east–to–west and west–to–east great circle paths across the south Caspian basin showing that this is not a site or instrumental effect. The top pair of seismograms in this figure show broadband vertical component seismograms, the middle pair show the waveforms low–passed at 22 mHz, and the bottom pair show the waveforms high–passed at 22 mHz. All waveforms are plotted on the same time scale and each of the pairs are plotted on the same amplitude scale. In each case the upper seismogram of each pair is the input to the basin and the lower is the output. There is a well–developed surface wave train for the waveform entering the basin but the intermediate frequency surface waves are largely missing from the surface wave train emerging from the basin only 450 km away. The low frequency surface waves are not significantly affected. This has been observed for both eastward and westward propagating surface waves, which are affected in the same manner.

We have modeled the response of the surface wave to this low–velocity sediment, deep basin structure and crustal thinning using a hybrid normal mode/finite difference approach. In these synthetic test we have used an idealized rendition of the south Caspian basin model shown in Fig. 1. The background model consist of a single layer 38 km thick crust with shear wave velocity 3.7 km s^{-1} overlying a 4.7 km s^{-1} mantle extending to 450.5 km depth. The basin consists of of four layers: a 2.625–km thick water layer, a 14.5–km thick sedimentary layer with shear wave velocity 2.0 km s^{-1} and shear wave Q of 25 in the upper 7 km of sediment and 50 in the lower 7.5 km, an 18–km thick crystalline crust with shear wave velocity 4.3 km s^{-1} and shear wave Q of 500, and a mantle upwarp 3–km thick. The near basin edge is at 381 km from the edge of the input grid and the far edge is at 762 km. The synthetic input is calculated using mode summation and the source is 2000 km outside the input grid. Synthetics seismograms are computed at a 50 km interval across the model at the solid–air or solid–water interface.

The true amplitude synthetic record section in Fig. 4 shows the vertical component seismograms spaced at 50 km intervals across the model. As the wave train passes into the basin [at 380 km distance] there is a significant increase in amplitude due to the impedance mismatch between the high velocity rocks outside the basin and the low velocity sediment within the basin. There are also small amplitude converted body waves in the basin [not seen on this scale] and reflected surface waves back into the crystalline crust on the left. As the wave train propagates through the basin the waveform is spread out in time due to the increased dispersion, and reduced in amplitude due to attenuation. As the wave train passes out of the basin [760 km distance] there is a reduction in amplitude of the waveform and a second surface wave reflected back into the basin. Fig. 5 compares the synthetic seismograms just before entering and just after exiting from the basin. The upper pair compare the broadband waveforms and the lower pair compare the long period waveforms (< 20 mHz). Each of the pairs have the same amplitude scale but there is a different amplitude scale between the pairs. As in the case of the observed surface wave trains, the synthetic surface wave show a pronounced attenuation of the intermediate period waves and only a small affect on the long period waves. This demonstrates that much of the observed surface wave train degradation can be modeled with the 2–D basin structure.

To gain some insight into the features of the basin which result in the anomalous surface wave propagation we have varied various parameters of the basin model and computed synthetic seismogram record sections for comparison with the seismograms in Fig. 4. We have varied the amount of mantle upwarp, removed the water layer, varied the shape of the boundaries, and varied the thickness and shear wave Q of the sediments. Of these parameters, the intermediate period surface waves are most severely affected by the sediment thickness and shear wave attenuation.

CONCLUSIONS AND RECOMMENDATIONS

The south Caspian basin is known to block L_g waves. We have observed a pronounced degradation of intermediate surface waves propagating across the south Caspian basin. We have begun to model these effects with hybrid normal mode/finite difference synthetics and sediment thickness and shear wave attenuation appear to be the dominate factors affecting the surface wave propagation. We intend to complete the modeling of the intermediate period surface waves, and then extend these calculations to higher frequencies and to the L_g phase.

REFERENCES

Brune, J.N., J.E. Nafe, and J.E. Oliver, A simplified method for the analysis and synthesis of dispersed wave trains, *J. Geophys. Res.*, *65*, 287, 1960.

Gomberg, J.S., K. Priestley, T.G. Masters, and J.N. Brune, The structure of the crust and upper mantle of northern Mexico. *Geophys. J. 94*, 1–20, 1988.

Kadinsky–Cade, K., M. Barazangi, J. Oliver, and B. Isacks, Lateral variations of high frequency seismic wave propagation at regional distances across the Turkish and Iranian Plateaus, *J. geophys. Res.*, *86*, 9377–9396, 1981

Mangino, S.G., and K. Priestley, The crust and upper mantle structure of the southern Caspian region, submitted to *Geophys. J. Int.*, 1997.

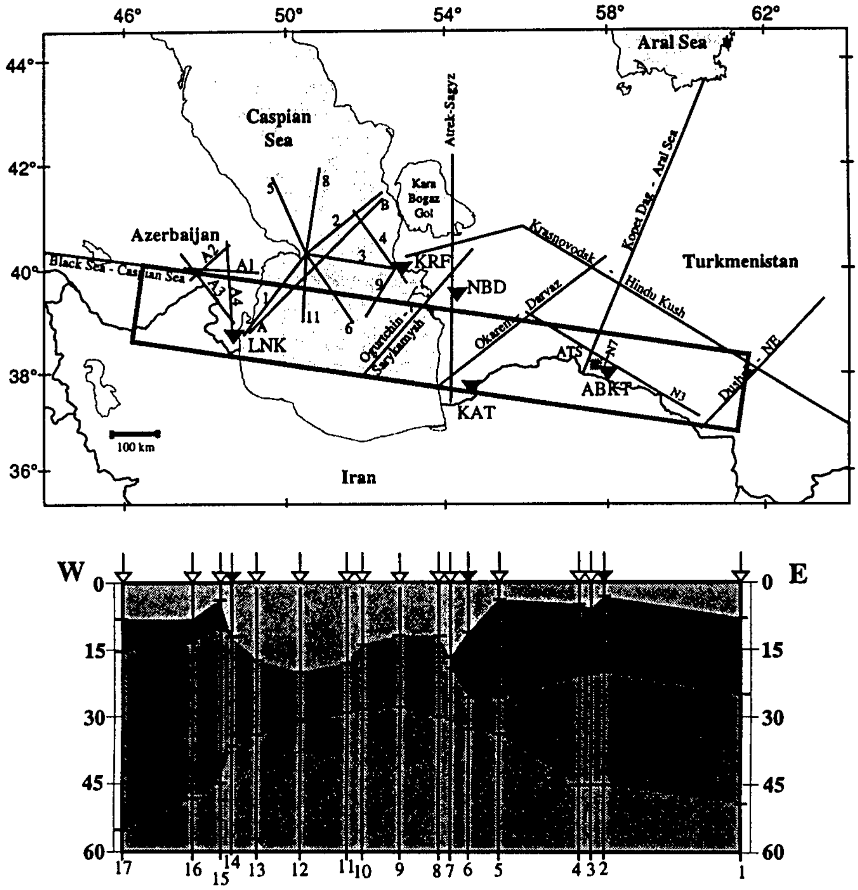

Figure 1: Cross-section of the crust and uppermost mantle (lower panel) beneath the region denoted by the box in the upper panel. Three principal crustal layers are characterized by their P–wave velocities: sediment and consolidated sediment (Vp < 4.8 km s^{-1}), "granitic" (Vp between 4.8–6.4 km s^{-1}), and upper mantle (Vp ≥ 8.0 km s^{-1}).

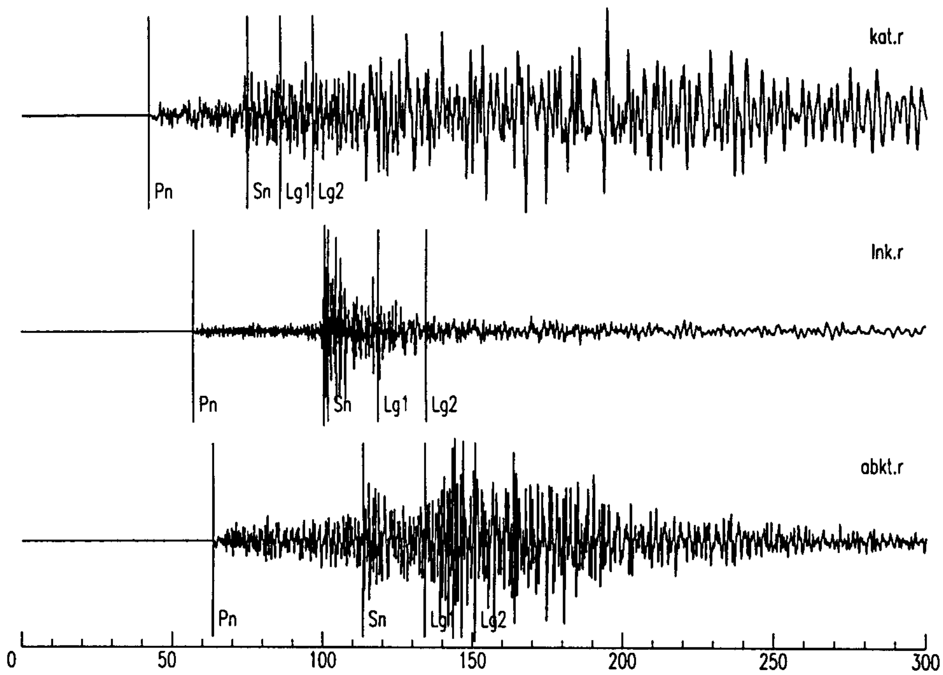

Figure 2: Radial component broadband seismograms for an earthquake occurring near KRF (Fig. 1) and recorded at KAT, LNK, and ABKT. The lines denoted by P_n and S_n indicate the IASPIE91 predicted arrival times for P_n and S_n , and the lines denoted by Lg1 and Lg2 correspond to group arrival times of 3.6 km s^{-1} and 3.2 km s^{-1} .

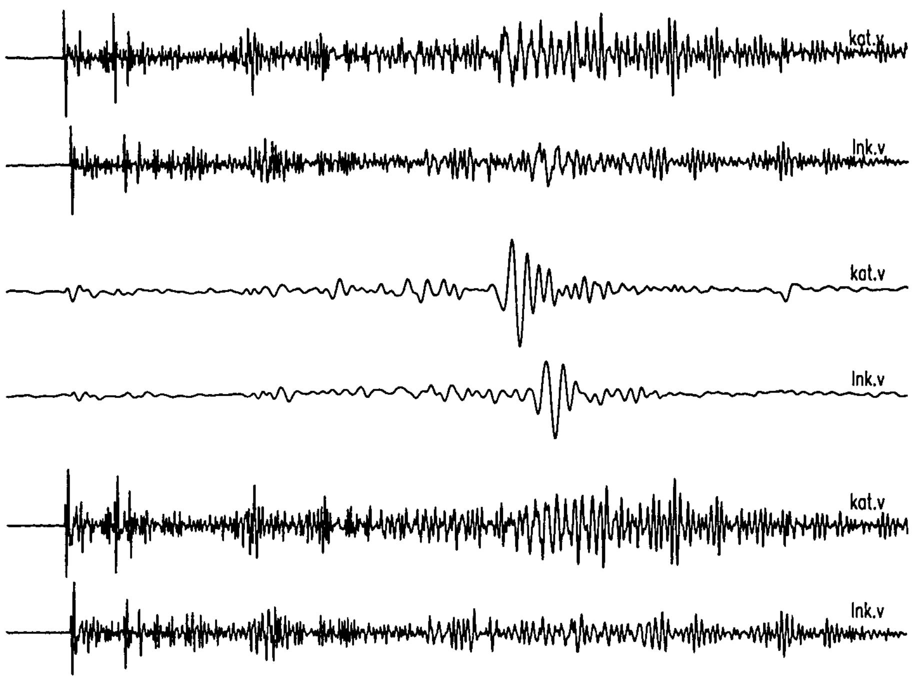

Figure 3: Seismograms from KAT and LNK (Fig. 1) of a teleseism propagating along the great circle path between the stations. The top pair of seismograms are the broadband recordings, the second pair have been lowpass–filtered at 0.022 Hz, and the bottom pair have been highpass–filtered at 0.022 Hz.

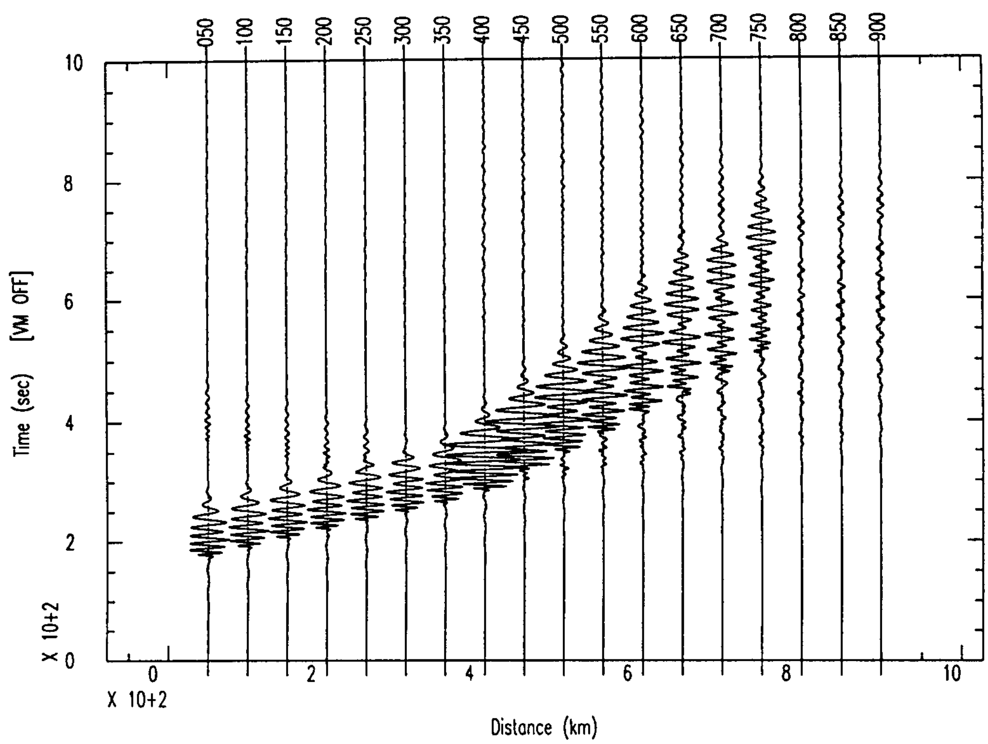

Figure 4: Record section of the finite difference synthetic seismograms across an idealized model of the south Caspian basin. The left edge of the basin is at 381 km and the right edge of the basin is at 762 km.

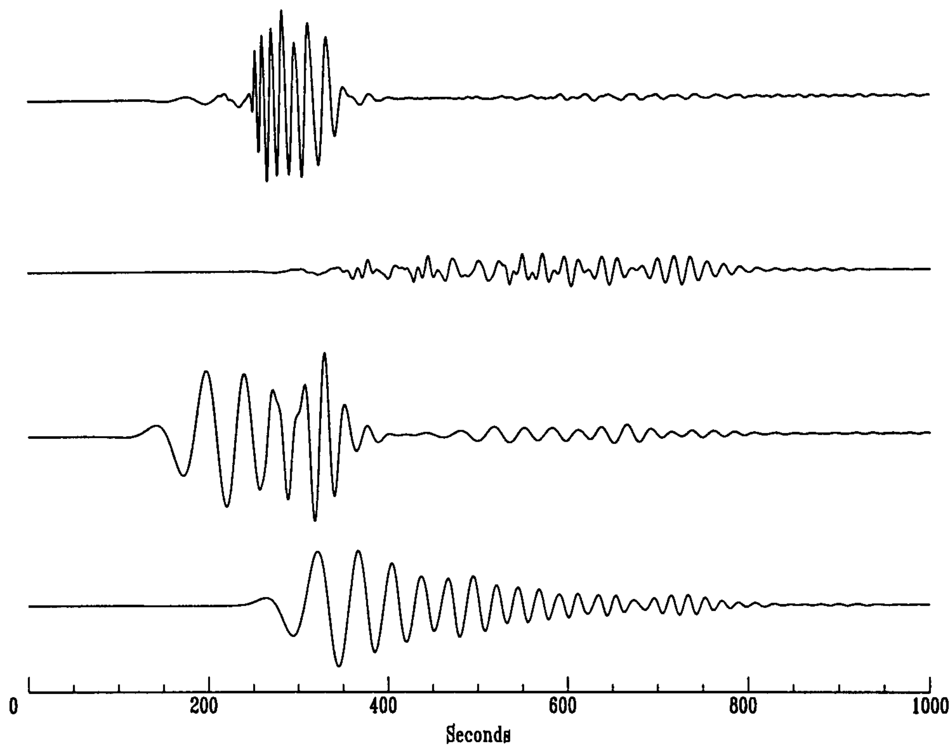

Figure 5: Comparison of broadband (upper pair) and lowpass filtered synthetic seismograms at distances of 300 and 800 km across the model.

M98000828

Report Number (14) LA-UR--97-2777

CONF-970967--

ᴾubl. Date (11) 199710

ˢponsor Code (18) DOE/DP, XF

ᴶC Category (19) UC-703, DOE/ER

DOE